2-D Angle Estimation in Beamspace Featuring Multidimensional Multirate Eigenvector Processing*

J. A. Gansman, M. D. Zoltowski and J. V. Krogmeier

School of Electrical Engineering, Purdue University, West Lafayette, IN 47907-1285, USA

ABSTRACT

Zoltowski and Kautz recently developed a beamspace domain based 1D angle estimation scheme for uniform linear arrays that allows one to solve for the arrival angles of plane waves via the roots of a small order polynomial and works with any type of front end beamformer. This paper extends their approach to the more general case of 2D angle estimation with a uniform rectangular array (URA) of sensors. The approach is based on the fact that the telescoped beamspace noise eigenvectors exhibit a bandpass characteristic. Therefore, multidimensional multirate processing can be performed to ultimately yield a small dimensional signal subspace. A novel version of ESPRIT can then be applied to effect closed-form 2D angle estimation and automatically couple the two components of the source directions. Simulations demonstrating the efficacy of the approach are presented.

1. INTRODUCTION

Two efficient methods for estimating the Direction of Arrival (DOA) of narrowband plane waves impinging upon a sensor array are Beamspace MUSIC [4] and ESPRIT [3]. While previous attempts to combine these methods have resulted in restrictive requirements on the beamformer, Zoltowski and Kautz [1] [2] recently developed a beamspace formulation of ESPRIT for 1D ULA's that works with any type of front end beamformer. The combined computational advantages of beamspace processing and ESPRIT make multidimensional DOA estimation a computationally feasible task.

This paper extends the new approach to the more general case of 2D angle estimation with a uniform rectangular array (URA). The approach is based on the observation that the beamspace noise eigenvectors can be transformed to vectors in the element noise subspace which are bandpass. Multidimensional multirate processing is then employed to ultimately yield a small dimensional signal subspace. A novel version of ESPRIT that estimates the two components of a source direction from an eigenvalue-eigenvector pair is then applied to this signal subspace.

The algorithm presented has two imporatant features. First, due to the linearity of 2D filtering and 2D decimation, the actual algorithm need only premultiply the beamspace signal eigenvectors by a precomputed transformation matrix. Second, the two components of a source direction are estimated from a single eigenvalue-eigenvector pair, so they are automatically coupled.

*This work was supported by AFOSR under contract no. F49620-92-J-0198 in conjunction with Wright Laboratories.

2. ARRAY GEOMETRY

The array geometry (Figure 1) consists of a planar $M \times N$ rectangular array of isotropic sensor elements with uniform half wavelength spacing. A narrowband signal with center frequency ω_o impinging upon the array with azimuth angle θ, measured from the x axis, and elevation angle ϕ, measured from the z axis, will encounter a phase delay of $\exp\{j\pi(k\cos\theta\sin\phi + l\sin\theta\sin\phi)\}$ when propagating between the origin and the k,l^{th} sensor. Assuming that the signal impinges from above the array, $\theta \in [-\pi, \pi]$ and $\phi \in [0, \frac{\pi}{2}]$, and defining the spatial frequency variables

$$\begin{aligned} \mu &= \pi\cos\theta\sin\phi \in [-\pi, \pi] \\ \nu &= \pi\sin\theta\sin\phi \in [-\pi, \pi] \end{aligned} \quad (1)$$

yields an element space array manifold of the form

$$\mathbf{A}_{MN}(\mu,\nu) = \mathbf{a}_M(\mu)\mathbf{a}_N^T(\nu), \quad (2)$$

where $\mathbf{a}_M(\mu)$ and $\mathbf{a}_N(\nu)$ are the one dimensional uniform linear array (ULA) manifold vectors.

$$\begin{aligned} \mathbf{a}_M(\mu) &\triangleq \left[1, e^{j\mu}, \ldots, e^{j(M-1)\mu}\right]^T \\ \mathbf{a}_N(\nu) &\triangleq \left[1, e^{j\nu}, \ldots, e^{j(N-1)\nu}\right]^T \end{aligned} \quad (3)$$

The m^{th} snapshot of the array due to d impinging signals can be written as

$$\mathbf{X}(m) = \sum_{i=0}^{d-1} s_i(m)\mathbf{A}_{MN}(\mu_i,\nu_i) + \mathbf{N}(m), \quad (4)$$

where $\mathbf{N}(m)$ is an $M \times N$ matrix of measurement noise associated with the m^{th} array snapshot.

The array response can be viewed as a vector as well as a matrix. Conversion between these forms is accomplished through the operators *vec*, that maps an $M \times N$ matrix to an $MN \times 1$ vector by concatenating its columns, and the inverse operator *mat*, that maps an $MN \times 1$ vector to an $M \times N$ matrix by using M consecutive elements of the vector for each column of the resulting matrix. In vector form, the array response is

$$\mathbf{x}(m) = \mathcal{A}_{MN}\mathbf{s}(m) + \mathbf{n}(m), \quad (5)$$

where $\mathbf{s}(m)$ is the vector of signal amplitudes, $\mathbf{a}_{MN}(\mu,\nu)$ is the array manifold in vector form, and the columns of $\mathcal{A}_{MN}$ are the signal steering vectors.

$$\begin{aligned} \mathbf{s}(m) &= [s_0(m), \ldots, s_{d-1}(m)]^T & (6)\\ \mathbf{a}_{MN}(\mu,\nu) &= vec(\mathbf{A}_{MN}(\mu,\nu)) = \mathbf{a}_N(\nu)\otimes\mathbf{a}_M(\mu) & (7)\\ \mathcal{A}_{MN} &= [\mathbf{a}_{MN}(\mu_0,\nu_0) \mid \ldots \mid \mathbf{a}_{MN}(\mu_{d-1},\nu_{d-1})] & (8)\end{aligned}$$

The d dimensional element space signal subspace is defined as the column-space of $\mathcal{A}_{MN}$, $\mathcal{S}_e \triangleq \mathcal{R}\{\mathcal{A}_{MN}\}$, and the $MN-d$ dimensional element space noise subspace is defined as the orthogonal complement of $\mathcal{S}_e$.

3. BEAMFORMING

For the class of separable two dimensional beamformers, the beamforming operation can be modeled as $\mathbf{Y}(m) = \mathbf{W}_\mu^H\mathbf{X}(m)\mathbf{W}_\nu^*$, where $\mathbf{W}_\mu$ and $\mathbf{W}_\nu$ are arbitrary $M\times M_b$ and $N\times N_b$ beamforming matrices for the μ and ν spatial frequencies respectively. The beamspace array snapshot vector is

$$\mathbf{y}(m) = \mathcal{B}\mathbf{s}(m) + \mathbf{n}_B(m) \quad (9)$$

and the beamspace array manifold is described by

$$\begin{aligned} \mathbf{b}(\mu,\nu) &= \left[\mathbf{W}_\nu^H \otimes \mathbf{W}_\mu^H\right]\mathbf{a}_{MN}(\mu,\nu) & (10)\\ \mathcal{B} &= [\mathbf{b}(\mu_0,\nu_0) \mid \ldots \mid \mathbf{b}(\mu_{d-1},\nu_{d-1})]. & (11)\end{aligned}$$

The d dimensional beamspace signal subspace, $\mathcal{S}_b$, is the column-space of $\mathcal{B}$, and the M_bN_b-d beamspace noise subspace is the orthogonal complement of $\mathcal{S}_b$.

If the measurement noise is zero mean, uncorrelated between sensors, and has equal power σ^2, and the beams are orthonormal, then the beamspace autocorrelation matrix is

$$\mathbf{R}_y = \mathcal{B}\mathbf{R}_s\mathcal{B}^H + \sigma^2\mathbf{I}. \quad (12)$$

The eigenvectors of $\mathbf{R}_y$ corresponding to the d largest eigenvalues $\{\mathbf{f}_i : i = 0,\ldots,d-1\}$ form a basis for $\mathcal{S}_b$ and as such are termed the "beamspace signal eigenvectors". The remaining eigenvectors $\{\mathbf{f}_j : j = d,\ldots,M_bN_b-1\}$ form a basis for $\mathcal{S}_b^\perp$ and are referred to as the "beamspace noise eigenvectors".

Since the noise eigenvectors lie in $\mathcal{S}_b^\perp$, they are orthogonal to the beamspace signal steering vectors, i.e., $\mathbf{b}^H(\mu_i,\nu_i)\mathbf{f}_j = 0$ for all $i = 0,\ldots d-1$ and $j = d,\ldots M_bN_b-1$. The general MUSIC algorithm exploits this orthogonality by forming the beamspace MUSIC null spectrum.

$$\begin{aligned} S_B(\mu,\nu) &= \sum_{j=d}^{M_bN_b-1}\left|\mathbf{b}^H(\mu,\nu)\mathbf{f}_j\right|^2\\ &= \sum_{j=d}^{M_bN_b-1}\left|\mathbf{a}_M^H(\mu)\mathbf{W}_\mu\mathbf{F}_j\mathbf{W}_\nu^T\mathbf{a}_N^*(\nu)\right|^2 \quad (13)\end{aligned}$$

where $\mathbf{F}_j$ is the beamspace noise eigenvector written in matrix form. Signal directions are estimated from values of μ and ν corresponding to nulls in $S_B(\mu,\nu)$.

4. MULTIRATE EIGENVECTOR PROCESSING

The MUSIC algorithm is built around the two dimensional Discrete Space Fourier Transform of the telescoped [2] beamspace noise eigenvectors

$$G_j(\mu,\nu) \triangleq \mathbf{a}_M^H(\mu)\mathbf{G}_j\mathbf{a}_N^*(\nu) = \mathbf{a}_M^H(\mu)\mathbf{W}_\mu\mathbf{F}_j\mathbf{W}_\nu^T\mathbf{a}_M^*(\nu). \quad (14)$$

Since $\mathbf{W}_\mu$ and $\mathbf{W}_\nu$ form beams in the desired subband, $G_j(\mu,\nu)$ is a bandpass function of μ and ν. If the M_bN_b beams encompass the spatial subband defined by $\{(\mu,\nu) : |\mu| \le \pi\left(\frac{M_b}{M}\right), |\nu| \le \pi\left(\frac{N_b}{N}\right)\}$ and have sufficiently low out of band sidelobes, the beamformer response will be negligible outside the subband of interest. Therefore, $\mathbf{G}_j$ can be decimated by $d_x = \frac{M}{M_b}$ and $d_y = \frac{N}{N_b}$ without incurring a significant amount of aliasing.

Decimating $\mathbf{G}_j$ is modeled as premultiplying and postmultiplying by the $M_b\times M$ and $N\times N_b$ decimation matrices $\mathbf{D}_x$ and $\mathbf{D}_y^T$ respectively. For example if $M_b = 2$ and $M = 6$

$$\mathbf{D}_x = \begin{bmatrix} 1 & 0 & 0 & 0 & 0 & 0\\ 0 & 0 & 0 & 1 & 0 & 0\end{bmatrix}.$$

The decimated telescoped beam space noise eigenvectors are given by

$$\mathbf{h}_j = [(\mathbf{D}_y\mathbf{W}_\nu)\otimes(\mathbf{D}_x\mathbf{W}_\mu)]\mathbf{f}_j. \quad (15)$$

Since decimation is a linear operation, it can be performed apriori on the telescoping matrices. The space spanned by the decimated telescoped beamspace noise eigenvectors will be referred to as $\mathcal{S}_d^\perp$.

Since $\mathbf{H}_j$ is $M_b\times N_b$, it has a 2D-DSFT given by $H_j(\mu,\nu) = \mathbf{a}_{M_b}^H(\mu)\mathbf{H}_j\mathbf{a}_{N_b}^*(\nu)$. From standard Multirate analysis [6], $H_j(\mu,\nu)$ and $G_j(\mu,\nu)$ are related by

$$H_j(\mu,\nu) = \frac{1}{d_xd_y}\sum_{p=0}^{d_x-1}\sum_{q=0}^{d_y-1}G_j\left(\frac{\mu-2\pi p}{d_x},\frac{\nu-2\pi q}{d_y}\right). \quad (16)$$

Since the beamformer response is negligible outside the subband, $H_j(\mu,\nu) \approx \frac{1}{d_xd_y}G_j\left(\frac{\mu}{d_x},\frac{\nu}{d_y}\right)$ over $-\pi \le \mu,\nu \le \pi$ and

$$H_j(d_x\mu_i, d_y\nu_i) = \frac{G_j(\mu_i,\nu_i)}{d_xd_y} = \frac{\mathbf{b}^H(\mu_i,\nu_i)\mathbf{f}_j}{d_xd_y} = 0. \quad (17)$$

This shows that the decimation process preserves the in band source nulls and increases their separation by the decimation factors d_x and d_y. Hence, the beamspace MUSIC null spectrum (13) could be reformulated as

$$S_B(\mu,\nu) = \sum_{j=d}^{M_bN_b-1}\left|\mathbf{a}_{M_b}^H(\mu)\mathbf{H}_j\mathbf{a}_{N_b}^*(\nu)\right|^2 \quad (18)$$

thereby reducing the computational intensity of each evaluation of $S_B(\mu,\nu)$.

For the 1D-ULA, this search is removed by defining $z = e^{j\mu}$ and writing S_B as a polynomial in z. Signal directions are then obtained from the roots of S_B. This procedure, referred to as Root-MUSIC [4], has always been theoretically possible for the 2D-URA, but the lack of 2D rooting algorithms has precluded its use in practice. However the efficient 2D rooting algorithm recently proposed by Hatke [7] has made 2D Root-MUSIC a viable option.

Alternatively, notice that

$$0 = H_j(d_x\mu_i, d_y\nu_i) = \mathbf{a}^H_{M_bN_b}(d_x\mu_i, d_y\nu_i)\mathbf{h}_j \tag{19}$$

for all $i = 0, \ldots, d-1$ and $j = d, \ldots, M_bN_b - 1$. Therefore, the decimated telescoped noise eigenvectors form a complete basis for a lower dimensional element space noise subspace $\mathcal{S}_d^{\perp}$, and the orthogonal complement, $\mathcal{S}_d$, is a lower dimensional element space signal subspace. This space will be referred to as *the decimated signal subspace*, even though it is not obtained by decimating the signal subspace.

5. 2D MULTIRATE ESPRIT

The ESPRIT algorithm requires an array formed by "sensor doublets" that are separated by a constant displacement vector [3]. This can be accomplished by viewing the $M_b \times N_b$ rectangular array as two overlapping $M_b \times (N_b - 1)$ subarrays with $M_b(N_b - 2)$ common elements. The resulting subarray manifolds are given by the first and last $N_b - 1$ columns of $\mathbf{A}_{M_bN_b}(\mu, \nu)$. Mathematically this is modeled as $\mathbf{A}_{M_bN_b}(\mu,\nu)\mathbf{\Gamma}_1$ and $\mathbf{A}_{M_bN_b}(\mu,\nu)\mathbf{\Gamma}_2$, where $\mathbf{\Gamma}_1$ and $\mathbf{\Gamma}_2$ are the first and last $N_b - 1$ columns of the $N_b \times N_b$ identity matrix. It is easily verified that the two subarray manifolds are related as

$$\mathbf{J}_2\mathbf{a}_{M_bN_b}(\mu,\nu) = e^{j\nu}\mathbf{J}_1\mathbf{a}_{M_bN_b}(\mu,\nu), \tag{20}$$

where $\mathbf{J}_1 \triangleq \mathbf{\Gamma}_1^T \otimes \mathbf{I}_{M_b}$ and $\mathbf{J}_2 \triangleq \mathbf{\Gamma}_2^T \otimes \mathbf{I}_{M_b}$. Therefore, the signal steering vectors for the subarrays are related by $\mathbf{J}_2\mathbf{a}_{M_bN_b}(d_x\mu_i, d_y\nu_i) = e^{jd_y\nu_i}\mathbf{J}_1\mathbf{a}_{M_bN_b}(d_x\mu_i, d_y\nu_i)$ and consequently

$$\mathbf{J}_2\mathcal{A}_{M_bN_b} = \mathbf{J}_1\mathcal{A}_{M_bN_b}\mathbf{\Upsilon}_\nu \tag{21}$$

where $\mathbf{\Upsilon}_\nu = \mathrm{diag}\{e^{jd_y\nu_0}, \ldots, e^{jd_y\nu_{d-1}}\}$. To generalize this to an arbitrary basis for for $\mathcal{S}_d$, let $\mathbf{K} = \mathcal{A}_{M_bN_b}\mathbf{T}$ for some $d \times d$ nonsingular matrix $\mathbf{T}$ and postmultiply by $\mathbf{T}$. This yields

$$\mathbf{J}_2\mathbf{K} = \mathbf{J}_1\mathbf{K}\mathbf{\Psi}, \tag{22}$$

where $\mathbf{\Psi} = \mathbf{T}^{-1}\mathbf{\Upsilon}\mathbf{T}$. This relationship is the basis for the TLS-ESPRIT algorithm [3]. It shows that the ν spatial frequencies can be estimated from the eigenvalues of the matrix that rotates the first $M_b(N_b-1)$ rows of $\mathbf{K}$ into the last $M_b(N_b-1)$ rows of $\mathbf{K}$.

Similarly, if the array is divided in a row-wise fashion the μ spatial frequencies can be estimated from the eigenvalues of the matrix that rotates $\mathbf{J}_3\mathbf{K}$ into $\mathbf{J}_4\mathbf{K}$, where $\mathbf{J}_3 = \mathbf{I}_{N_b} \otimes \mathbf{\Gamma}_3$, $\mathbf{J}_4 = \mathbf{I}_{N_b} \otimes \mathbf{\Gamma}_4$, and $\mathbf{\Gamma}_3$ and $\mathbf{\Gamma}_4$ are the first and last $M_b - 1$ rows of the $M_b \times M_b$ identity matrix. However, if the μ and ν frequencies are obtained independently in this fashion, there is no apparent way to pair the frequency components corresponding to a specific signal.

To circumvent this problem, notice that as long as no two signals have the same μ and ν frequencies, $\mathbf{J}_1\mathbf{K}$ and $\mathbf{J}_2\mathbf{K}$ are rank d. Therefore, $\mathbf{\Psi}$ always exists and has a full set of eigenvalues and linearly independent eigenvectors. Consider performing an eigenvalue decomposition of $\mathbf{\Psi}$ to obtain $\mathbf{\Psi} = \mathbf{E}\mathbf{\Upsilon}\mathbf{E}^{-1}$.

If ν_i is a distinct frequency, then $e^{jd_y\nu_i}$ is a distinct eigenvalue of $\mathbf{\Psi}$ and the associated right eigenvector is unique (to within a scalar multiple). Therefore, $\mathbf{e}_i$ is the i^{th} column of $\mathbf{T}^{-1}$ and the i^{th} signal steering vector can be obtained as

$$\mathbf{K}\mathbf{e}_i = \mathcal{A}_{M_bN_b}\mathbf{T}\mathbf{e}_i = \alpha_i\mathbf{a}_{M_bN_b}(d_x\mu_i, d_y\nu_i). \tag{23}$$

The μ frequency is obtained from the steering vector by letting $\mathbf{l}_i = \mathbf{K}\mathbf{e}_i$ and noticing that

$$\tfrac{1}{(M_b-1)N_b}\,(\mathbf{J}_3\mathbf{l}_i)^H\,(\mathbf{J}_4\mathbf{l}_i) = e^{jd_x\mu_i}. \tag{24}$$

An important observation is that the μ and ν frequencies for a signal are estimated from an eigenvalue-eigenvector pair and as such are automatically coupled.

If ν_i is not a distinct frequency, say $\nu_0 = \ldots = \nu_{p-1}$, then $\mathbf{\Psi}$ has an eigenvalue of multiplicity p and the associated eigenvectors $\{\mathbf{e}_0, \ldots, \mathbf{e}_{p-1}\}$, are not unique. Therefore, $\mathbf{e}_i$ is not the i^{th} column of $\mathbf{T}^{-1}$. However,

$$\begin{aligned}&\mathbf{K}\,[\mathbf{e}_0 \mid \ldots \mid \mathbf{e}_{p-1}] = \\ &[\mathbf{a}_{M_bN_b}(d_x\mu_0, d_y\nu_0) \mid \ldots \mid \mathbf{a}_{M_bN_b}(d_x\mu_{p-1}, d_y\nu_{p-1})]\,\mathbf{C}\end{aligned} \tag{25}$$

for some $p \times p$ matrix $\mathbf{C}$. This has the ESPRIT structure, and applying ESPRIT in a row-wise fashion will yield the μ frequencies. Coupling the frequencies is not an issue because the corresponding ν frequencies are identical.

Several aspects of the above development need to be emphasized. First, the matrix products $\mathbf{J}_1\mathbf{K}$ and $\mathbf{J}_2\mathbf{K}$ are the first and last $M_b(N_b-1)$ rows of $\mathbf{K}$, and can be effected without performing any matrix multiplies. Second, the rotation matrix $\mathbf{\Psi}$ is estimated by applying the Total Least Squares method of Golub and Van Loan [5] (as in [3]). Finally, equation (22) has a unique solution for $\mathbf{\Psi}$ provided that the number of rows exceeds (or equals) the number of columns in $\mathbf{J}_1\mathbf{K}$. Since $\mathbf{J}_1\mathbf{K}$ $M_b(N_b-1) \times d$, TLS-ESPRIT can determine up to $M_b(N_b-1)$ signal directions.

6. BANDLIMITING THE RESPONSE

Thus far it has been assumed that beamformer employed is comprised of M_bN_b beams that encompass the subband defined by $-\pi\left(\frac{M_b}{M}\right) \le \mu \le \pi\left(\frac{M_b}{M}\right)$ and $-\pi\left(\frac{N_b}{N}\right) \le \nu \le \pi\left(\frac{N_b}{N}\right)$. If the beams are insufficiently bandlimited or not centered at broadside, the beamspace noise eigenvectors can be modulated to baseband and filtered prior to decimation to make the assumption valid. While the filtering process increases the length of the eigenvectors, Kautz [1] showed that a decimated version of the filter can be deconvolved from the decimated telescoped eigenvectors to remove most of this extra dimensionality. In the 1D case this yields a $d+1$ dimensional decimated signal subspace. Therefore, the resulting $\mathbf{\Psi}$ matrix has an eigenvalue that is not related to a signal direction. Kautz argued that this extraneous eigenvalue is far removed from the unit circle, so it is easily identified and ignored. For a 2D-URA, the filtering is two dimensional, so after deconvolution $\mathbf{\Psi}$ has $M_b + N_b + 1$ extra eigenvalues. Kautz's argument is still valid, but now the eigenvalue decomposition is performed on a matrix that is $(d + M_b + N_b + 1) \times (d + M_b + N_b + 1)$ instead of $d \times d$. This nonnegligible increase in complexity can be easily circumvented by improving the front end beamformer.

7. REDUCTIONS IN COMPLEXITY

Two additional reductions in the algorithm are possible. First, placing the reference point in the center of the array yields array manifold vectors of the form $\mathbf{A}_{MN}(\mu,\nu) = \mathbf{a}_M(\mu)\mathbf{a}_N^T(\nu)$, where

$$\mathbf{a}_M(\mu) = \left[e^{-j(\frac{M-1}{2})\mu}, \ldots, e^{j(\frac{M-1}{2})\mu}\right]^T. \quad (26)$$

These steering vectors are conjugate centrosymmetric, i.e.,

$$\tilde{\mathbf{I}}_{MN}\mathbf{a}_{MN}(\mu,\nu) = \mathbf{a}_{MN}^*(\mu,\nu), \quad (27)$$

where $\tilde{\mathbf{I}}_M$ is the $M \times M$ reverse permutation matrix, that "flips" the $M\times 1$ column vector. Since $\tilde{\mathbf{I}}_M$ is its own inverse and $\tilde{\mathbf{I}}_{MN} = \tilde{\mathbf{I}}_N \otimes \tilde{\mathbf{I}}_M$, applying a conjugate centrosymmetric beamformer yields real valued beamspace steering vectors.

$$\mathcal{B} = \left[\mathbf{W}_\nu^H \otimes \mathbf{W}_\mu^H\right]\tilde{\mathbf{I}}_{MN}\tilde{\mathbf{I}}_{MN}\mathcal{A} = \mathcal{B}^* \quad (28)$$

Therefore, the real part of the beamspace correlation matrix

$$\mathcal{R}e\{\mathbf{R}_y\} = \mathcal{B}\,\mathcal{R}e\{\mathbf{R}_s\}\,\mathcal{B}^T + \sigma^2\mathbf{I} \quad (29)$$

has the desired eigen structure. Hence the TLS-ESPRIT algorithm can be applied to the real part, instead of the complex, correlation matrix (see [4]).

The second reduction is the method of obtaining $\mathbf{K}$. Thus far $\mathbf{K}$ has been obtained as the orthogonal complement of $\mathbf{H} = \mathbf{W}_t\mathbf{F}_n$ which requires a computationally intensive SVD. An alternatve basis for $\mathcal{S}_d$ can be obtained by applying a simple linear transformation to $\mathbf{F}_s$ (see [1]). To show this, let $\mathbf{Z} = \mathbf{W}_t\left(\mathbf{W}_t^H\mathbf{W}_t\right)^{-1}$ and notice that

$$(\mathbf{Z}\mathbf{f}_i)^H\mathbf{h}_j = \left[\mathbf{W}_t\left(\mathbf{W}_t^H\mathbf{W}_t\right)^{-1}\mathbf{f}_i\right]^H\mathbf{W}_t\mathbf{f}_j = \mathbf{f}_i^H\mathbf{f}_j = 0. \quad (30)$$

Hence, $\mathbf{Z}$ maps a beamspace signal eigenvector to the decimated signal subspace. Therefore K can be determined as

$$\mathbf{K} = [\mathbf{Z}\mathbf{f}_0 \mid \ldots \mid \mathbf{Z}\mathbf{f}_{d-1}]. \quad (31)$$

In the event that filtering is employed, this transformation yields an insufficient basis for $\mathcal{S}_d$. However the remaining basis vectors can be obtained by precomputing the orthogonal complement of $\mathbf{W}_t$.

8. ALGORITHM

1. Compute the beamforming and telescoping matrices:

$$\begin{aligned}\mathbf{W}_b &= \mathbf{W}_\nu \otimes \mathbf{W}_\mu\\ \mathbf{W}_t &= (\mathbf{D}_y\mathbf{W}_\nu)\otimes(\mathbf{D}_x\mathbf{W}_\mu)\\ \mathbf{Z} &= \mathbf{W}_t\left(\mathbf{W}_t^H\mathbf{W}_t\right)^{-1}.\end{aligned}$$

2. Store P snapshots of the array as the columns of $\mathbf{X}$, and form the beamspace snapshot $\mathbf{Y} = \mathbf{W}_b^H\mathbf{X}$.

3. Compute the EVD of the real part of the beamspace correlation matrix and form $\mathbf{K}$.

$$\begin{aligned}\mathcal{R}e\{\mathbf{R}_y\} &= \tfrac{1}{P}\,\mathcal{R}e\left\{\mathbf{Y}\mathbf{Y}^H\right\} = \sum_{i=0}^{M_bN_b-1}\lambda_i\mathbf{f}_i\mathbf{f}_i^H\\ \mathbf{K} &= \mathbf{Z}[\mathbf{f}_0 \mid \ldots \mid \mathbf{f}_{d-1}]\end{aligned}$$

4. Form $\mathbf{K}_{12} = [\mathbf{J}_1\mathbf{K} \mid \mathbf{J}_2\mathbf{K}]$, and compute the EVD of $\mathbf{K}_{12}^H\mathbf{K}_{12} = \mathbf{Q}\mathbf{\Lambda}\mathbf{Q}^{-1}$.

5. Partition $\mathbf{Q}$ into $d\times d$ upper and lower blocks and compute $\mathbf{\Psi} = -\mathbf{Q}_{12}(\mathbf{Q}_{22})^{-1}$.

6. Compute the EVD of $\mathbf{\Psi}$ to obtain $\mathbf{\Upsilon}$ and estimate the ν frequencies.

$$\mathbf{\Psi} = \mathbf{E}\mathbf{\Upsilon}\mathbf{E}^{-1} \quad \mathbf{\Upsilon} = \mathrm{diag}\{\gamma_0,\ldots,\gamma_{d-1}\} \quad \nu_i = \tfrac{1}{d_y}\arg\gamma_i$$

7. For distinct ν_i estimate the μ frequencies as $\mu_i = \frac{1}{d_x}\arg\rho_i$, where $\rho_i = \mathbf{l}_i^H\mathbf{P}\mathbf{l}_i$, $\mathbf{l}_i = \mathbf{K}\mathbf{e}_i$, and $\mathbf{P} = \frac{1}{(M_b-1)N_b}\left[\mathbf{I}_N \otimes \left(\mathbf{\Gamma}_3^T\mathbf{\Gamma}_4\right)\right]$.

8. For repeated ν_i form $\mathbf{L} = \mathbf{K}[\mathbf{e}_1 \mid \ldots \mid \mathbf{e}_{p-1}]$ and estimate the μ frequencies as $\mu_i = \frac{1}{d_x}\arg\rho_i$, where ρ_i are the eigenvalues of the matrix that rotates the $\mathbf{J}_3\mathbf{L}$ into $\mathbf{J}_4\mathbf{L}$ (steps 4 - 6).

9. SIMULATIONS

Various computer simulations were performed to verify the proposed 2D Multirate ESPRIT algorithm. Unless stated otherwise, all simulations use a 32×32 array with half wavelength spacing and 3 sources with equal power σ_s^2. The beamspace correlation matrix is estimated from 32 snapshots of the array and 200 trials are executed for each particular point of interest. The front end beamformer consists of 64 beams centered at broadside. so the subband being probed is $-\frac{\pi}{4} \le \mu,\nu \le \frac{\pi}{4}$, and the maximal decimation rate of $d_x = d_y = 4$ is used. Three separate types of beams are simulated, DFT beams, Hamming beams and Orthonormal Hamming beams. The error criterion used to evaluate the algorithm is the average RMS error between the actual signal frequencies and their estimates, $\overline{\mathrm{rms}} = \frac{1}{d}\sum_{i=0}^{d-1}\sqrt{(\mu_i-\hat{\mu}_i)^2 + (\nu_i - \hat{\nu}_i)^2}$, and SNR refers to the per signal per element signal to noise ratio, $\mathrm{SNR} = 10\log\frac{\sigma_s^2}{\sigma_n^2}$.

Before simulating ESPRIT, it is worthwhile to simulate 2D Multirate Spectral MUSIC (18) (Figure 2). The three signals simulated had 0 dB SNR and spatial frequencies $(\alpha,-\alpha)$, $(-\alpha,-\alpha)$, and $(-\alpha,\alpha)$, where $\alpha = \frac{2\pi}{32} = 0.1963$. Since the main lobe width of the Hamming beams is $\frac{4\pi}{32}$, these signals are said to have full beam width separation. This shows that 2D Multirate processing does indeed work, and the resulting spectral nulls are moved to $(\pm d_x\alpha, \pm d_y\alpha) = (\pm 0.7852, \pm 0.7852)$. For comparison purposes Figure 3 contains a contour plot of the MUSIC spectrum, and a scatter plot of 2D Multirate ESPRIT with the same simulation parameters. Note that the scatter plot of ESPRIT has compensated for the d_x and d_y factors. Furthermore this plot verifies the automatic coupling properties of the proposed ESPRIT algorithm.

To investigate the SNR dependence of the estimator, the same three signals were simulated and the SNR was varied from -30dB to 0dB (Figure 4). This shows that at low SNR measurement noise dominates so DFT beams perform better, but at high SNR values aliasing due to large sidelobes dominates so Hamming beams perform better.

It is well known that the performance of 1D beamformers decay near the band edges. To see how the 2D beamformer performance varies with location in the subband, one signal was simulated and its position was varied from the center of the band to the band edge along the μ axis and along the $\mu = \nu$ diagonal (see Figure 5). The performance does indeed decay at the band edge, hence subbands should be overlapped.

10. CONCLUSION

This paper has presented a beamspace version of ESPRIT for uniform rectangular arrays that facilitates closed-form 2D angle estimation. Through the use of multidimensional multirate processing techniques, a simple transformation matrix is precomputed that when applied to the beamspace signal eigenvectors yields a small dimensional signal subspace. The two components of the source directions are then obtained from an eigenvalue-eigenvector pair, so they are automatically coupled. Simulations were presented that demonstrate the practicality of the algorithm.

REFERENCES

[1] G. M. Kautz and M. D. Zoltowski, "Beamspace DOA Estimation Featuring Multirate Eigenvector processing," *Submitted to IEEE Trans, on Signal Processing*, May. 1994.

[2] M. D. Zoltowski, J. V. Krogmeier, and G. M. Kautz, "Novel Multirate Processing of Beamspace Noise Eigenvectors," *Submitted to IEEE Signal Processing Letters*, Jan. 1994.

[3] R. Roy and T. Kailath, "ESPRIT-Estimation of Signal Parameters Via Rotational Invariance Techniques," *IEEE Trans. Acoust., Speech, Signal Processing*, vol. 37, no. 7, pp. 984-995, July 1989.

[4] M. D. Zoltowski, G. M. Kautz, and S. D. Silverstein, "Beamspace Root-MUSIC," *IEEE Trans. on Signal Processing*, vol. 41, no. 1, pp. 344-364, Jan. 1993.

[5] G. H. Golub and C. F. Van Loan, *Matrix Computations*. Baltimore. MD: Johns Hopkins University Press. 1984

[6] P. P. Vaidyanathan, *Multirate Systems and Filter Banks*, New Jersey: Prentice Hall, 1993.

[7] Gary F. Hatke, "A Class of Polynomail Rooting Algorithms for Joint Azimuth/Elevation Estimation Using Planar Arrays," *MIT Lincoln Labs* Project Memorandum No. 44PM-CMT-0002 Aug. 30, 1990

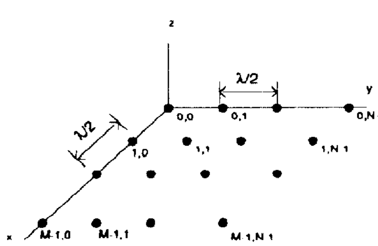

Figure 1: Array Geometry

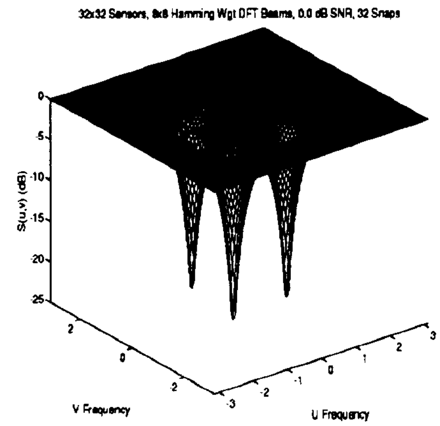

Figure 2: Beamspace MUSIC Null Spectrum: 3 sources, 8x8 Hamming Beams

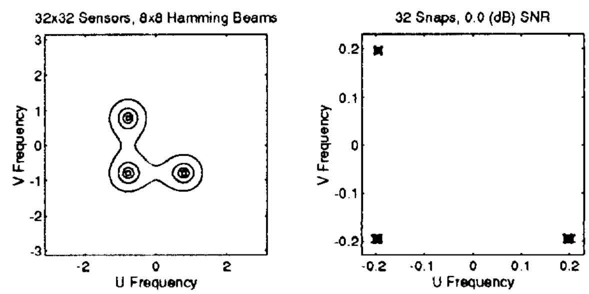

Figure 3: Left: Contour plot of MUSIC. Right: Scatter Plot of 2D ESPRIT for 0dB SNR and 8x8 Hamming Beams.

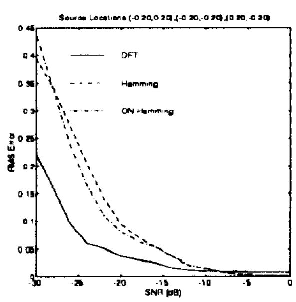

Figure 4: RMS Error vs SNR for 2D Multirate ESPRIT.

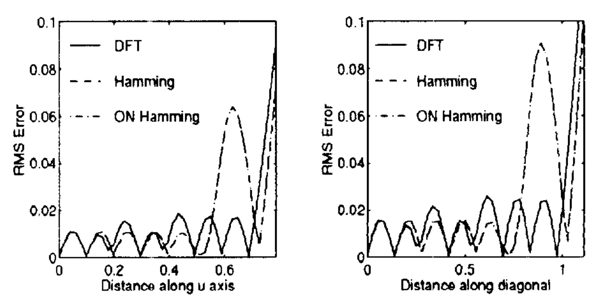

Figure 5: RMS Error vs Position along the μ axis (Left) and $\mu = \nu$ diagonal (Right) for 2D Multirate ESPRIT with 1 source and 0dB SNR.